Nitride Oxygenation

International Edition: DOI: 10.1002/anie.201908689
German Edition: DOI: 10.1002/ange.201908689

Conversion of a Fleeting Open-Shell Iron Nitride into an Iron Nitrosyl

Hao-Ching Chang, Yen-Hao Lin, Christophe Werlé, Frank Neese, Way-Zen Lee, Eckhard Bill,* and Shengfa Ye**

Dedicated to Prof. Wolfgang Kaim on the occasion of his retirement

Abstract: *Terminal metal nitrides have been proposed as key intermediates in a series of pivotal chemical transformations. However, exploring the chemical activity of transient tetragonal iron(V) nitrides is largely impeded by their facile dimerization in fluid solutions. Herein, in situ EPR and Mössbauer investigations are presented of unprecedented oxygenation of a paramagnetic iron(V) nitrido intermediate, $[Fe^{V}N(cyclam\text{-}ac)]^{+}$ (**2**, cyclam-ac^{-} = 1,4,8,11-tetraazacyclotetradecane-1-acetate anion), yielding an iron nitrosyl complex, $[Fe(NO)(cyclam\text{-}ac)]^{+}$ (**3**). Further theoretical studies suggest that during the reaction a closed-shell singlet O atom is transferred to **2**. Consequently, the N–O bond formation does not follow a radical coupling mechanism proposed for the N–N bond formation but is accomplished by three mutual electron-transfer pathways between **2** and the O atom donor, thanks to the ambiphilic nature of **2**.*

It is of fundamental importance to understand the structure–activity relationship of terminal metal nitrides (N^{3-}) because of their involvement in N_2 reduction[1] and NH_3 oxidation processes.[2] Among all transition metals, iron nitrides attract particular attention owing to their biological relevance.[1a,b] To date, a plethora of iron nitrides in various iron oxidation states have been synthesized, all featuring either tetragonal or trigonal symmetry.[3] Because most trigonal iron(IV/V) nitrides are isolable, presently the majority of reactivity investigations focus on these species, which indeed exhibit diversified reactivity.[3,4] For instance, treating such complexes with reducing agents was found to afford ammonia,[5] and they are typically capable of initiating nitrogen atom transfer to a range of nucleophiles.[5c,6] In contrast, all tetragonal iron(V/VI) nitrides are highly unstable and have to be prepared invariably under cryogenic conditions.[3] For example, in fluid solutions, $[Fe^{V}N(cyclam\text{-}ac)]^{+}$ (**2**, cyclam-ac^{-} = 1,4,8,11-tetraazacyclotetradecane-1-acetate anion) undergoes facile dimerization to eventually release N_2.[7] The nitrido ligands of tetragonal low-spin iron(V) nitrides feature considerable radical character, because their singly occupied molecular orbital (SOMO) is one of the two Fe–N π* molecular orbitals (MOs) formed by the antibonding combinations of the Fe $d_{xz/yz}$ and N $p_{x/y}$ atomic orbitals (Scheme 1).[8] In contrast,

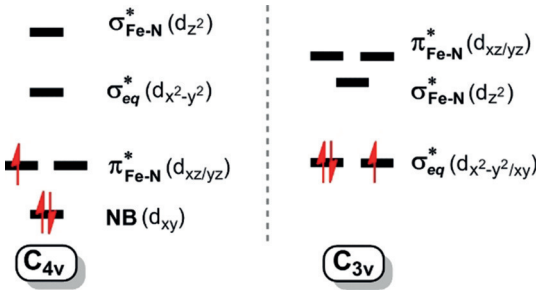

Scheme 1. Qualitative orbital splitting pattern for iron(V) nitrides (NB = non-bonding).

the SOMO of the corresponding trigonal species is either of the Fe $d_{x^2-y^2}$ or the Fe d_{xy} based MOs, both perpendicular to the Fe–N interaction.[9] Consequently, trigonal iron(V) nitrides are often more stable than their tetragonal analogues. The fleeting nature of the latter poses a challenge to explore their reactivity, and mass spectrometry[10] or time-resolved spectroscopy has to be relied upon.[11] Using these methods, tetragonal iron nitrides were shown to activate C–H and C=C bonds of organic substrates,[10,11] similar to their trigonal congeners.[12]

Complex **2** having an $S = 1/2$ ground state[13] exhibits an unusual electron paramagnetic resonance (EPR) spectrum with a slightly asymmetric zero-crossing derivative signal around $g_{\perp} = 1.7$ and a broad negative peak at $g_{\parallel} = 1$.[8] Recently, these highly anisotropic g values were shown to be a unique signature of tetragonal low-spin iron(V)

[*] Dr. H.-C. Chang, Prof. Dr. F. Neese, Dr. S. Ye
Max-Planck-Institut für Kohlenforschung
Kaiser-Wilhelm-Platz 1, 45470 Mülheim an der Ruhr (Germany)
E-mail: shengfa.ye@kofo.mpg.de
Homepage: http://www.kofo.mpg.de/ye
Y.-H. Lin, Prof. Dr. W.-Z. Lee
Department of Chemistry, National Taiwan Normal University
88, Ting-chou Rd. Sec. 4, 11677 Taipei (Taiwan)
E-mail: wzlee@ntnu.edu.tw
Dr. C. Werlé, Dr. E. Bill
Max-Planck-Institut für Chemische Energiekonversion
Stiftstrasse 34–36, 45470 Mülheim an der Ruhr (Germany)
E-mail: eckhard.bill@cec.mpg.de
Prof. Dr. W.-Z. Lee
Department of Medicinal and Applied Chemistry
Kaohsiung Medical University
100, Shi-Chuan 1st Rd., 807 Kaohsiung (Taiwan)
Supporting information and the ORCID identification number(s) for the author(s) of this article can be found under: https://doi.org/10.1002/anie.201908689.

nitrides.[8] Thus, EPR can be used as a sensitive and efficient tool to detect such transient intermediates, which opens up a new way to probe their chemical activity. Herein, we present in situ spectroscopic investigations of oxygenation of **2** to yield the corresponding nitrosyl species (Scheme 2b). Note

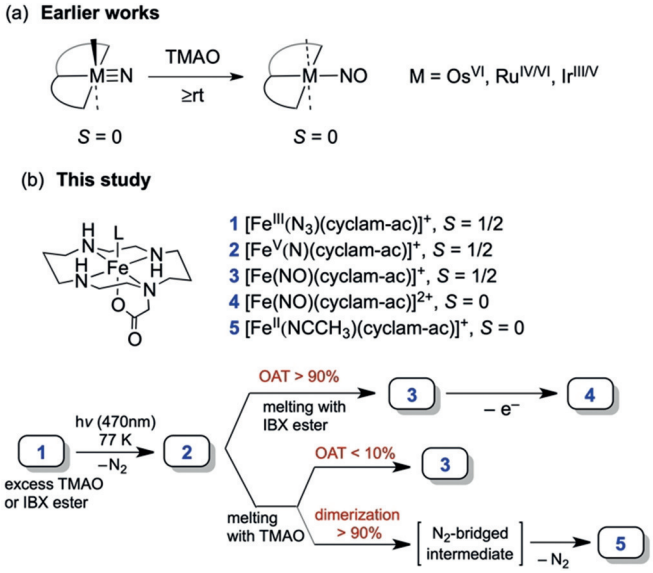

Scheme 2. Oxygenation of terminal metal nitrides.

that chemisorbed nitrogen atoms on metal surfaces are key intermediates of selective NH_3 oxidation for industrial NO production.[2] To the best of our knowledge, conversion of an open-shell metal nitride into a metal nitrosyl is unprecedented. Only oxygenation of diamagnetic 4d (ruthenium(IV/VI)[14]) and 5d (osmium(VI)[15] and iridium(III/V)[16]) metal nitrides has been reported (Scheme 2a), and, more importantly, the underlying mechanism remains poorly understood.

Complex **2** was generated by bulk photolysis of [Fe^{III}-(N_3)(cyclam-ac)](PF_6) (**1**) in frozen solutions with a yield of almost 100%, as revealed by EPR investigations (Figure 1a).[8] Upon thawing, **2** was found to decay rapidly via dimerization.[7] To intercept this pathway, a large excess of oxygen atom transfer (OAT) agents was mixed with **1** prior to freezing and illumination. During photolysis, the formation of **2** and its reaction with the OAT reactant in the solid matrix were monitored by repeated spectroscopic measurements of the frozen samples.

After one-hour irradiation of the frozen reaction mixture of 1 mM of **1** and 100 equiv of isopropyl 2-iodoxybenzoate (IBX-ester) in CH_3CN, the EPR spectrum revealed emergence of a new nearly isotropic signal centered at $g \approx 2$ attributed to new species **3**, along with some unreacted **2** (Figure 1b). Numerical integration showed that the total spin concentration remained unchanged and the relative amount of **3**:**2** was ca. 1:9. Upon thawing, the sample in a cold EtOH bath (−40 °C) and immediately refreezing it, **3** elicited a well-resolved hyperfine structure, concurrent with complete disappearance of the broad signal of **2** (Figure 1c, d). Remarkably, the EPR features of **3** match exactly those published for

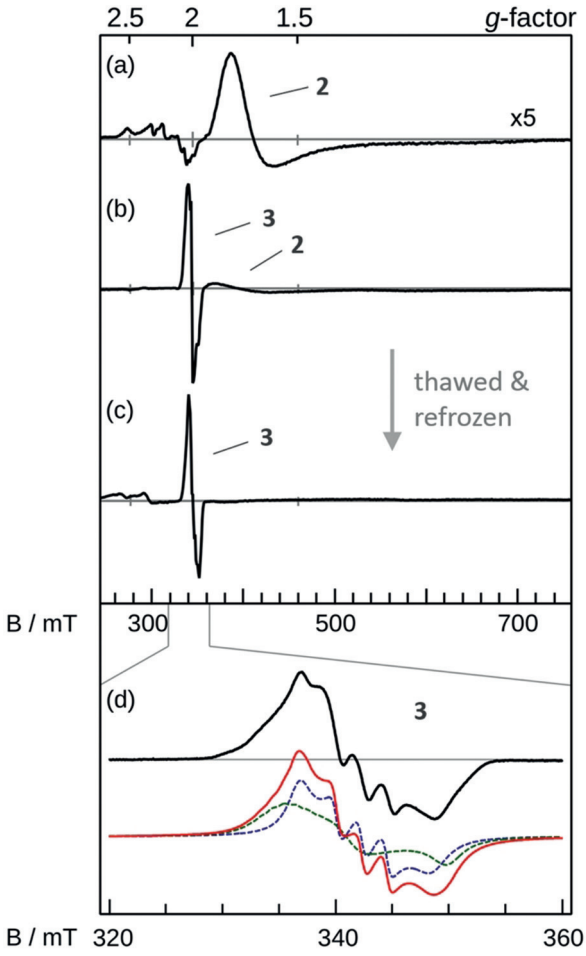

Figure 1. X-band EPR spectra of a) **2** at 10 K generated without IBX-ester; b) illuminated **1** with 100 equiv of IBX-ester; c) the same sample as for (b) after thawing and quick refreezing; d) the zoomed-in spectrum of (c). In black: experimental spectrum of **3**, red: simulation by superposition of two isomers given in green and blue (For details, see the Supporting Information).

[Fe(NO)(cyclam-ac)]$^+$,[17] a structurally and spectroscopically well-characterized $S = 1/2$ {Fe-NO}^{7} complex.[18] Control experiments demonstrated that IBX-ester is photostable under the experimental conditions. Spin quantifications revealed that the thawing process led to an approximate ten-fold decrease in the total spin concentration, and that the maximal yield of **3** is only 10% relative to **1**. We surmised that once formed, the majority of **3** converted into an EPR-silent species in the thawed reaction mixture.

To identify the EPR-silent product, the same reaction was performed with 50% ^{57}Fe-enriched **1** (5 mM) in CH_3CN. The 80 K zero-field Mössbauer spectrum of the frozen photolyzed reaction mixture is dominated by a highly asymmetric and broad doublet known for **2** (Figure 2a, isomer shift $\delta = 0.00\ mm\,s^{-1}$ and quadrupole splitting $|\Delta E_Q| = 1.72\ mm\,s^{-1}$).[7] Unfortunately, the Mössbauer spectrum of **3** ($\delta = 0.28\ mm\,s^{-1}$ and $|\Delta E_Q| = 0.85\ mm\,s^{-1}$) was also found to have a similar line shape.[17] Consequently, the overlap of the Mössbauer features of **2** and **3** renders quantification of **3** difficult. Careful simulation analyses indicated that before thawing the sample

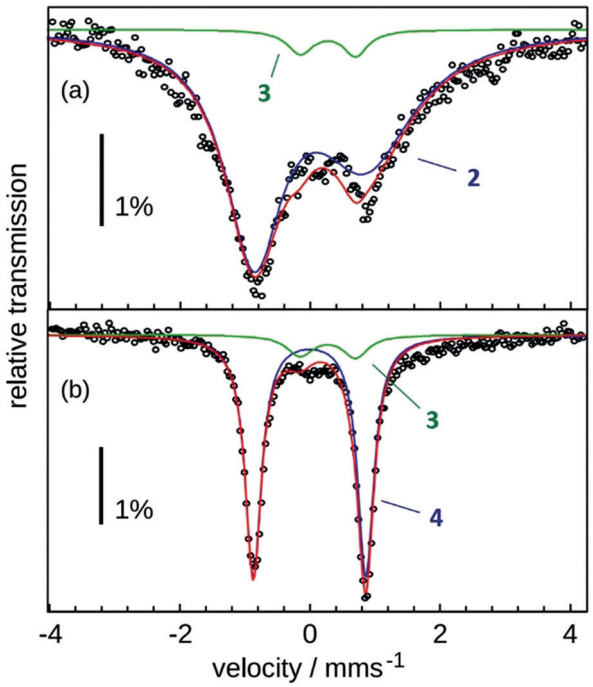

Figure 2. Mössbauer spectra of photolyzed **1** recorded at 80 K in the presence of 100 equiv of IBX-ester, a) before (**2**: blue; **3:** green) and b) after thawing the sample (**3:** green; **4**: blue). The simulated subspectrum of **3** accounts for 5% and 12% of the total iron content in (a) and (b), respectively.

contained at least 90% of **2** and less than 10% of **3** (Figure 2a; details given in the Supporting Information). Thawing at room temperature and refreezing the sample resulted in a well-resolved dominating (88%) quadrupole doublet (Figure 2b, $\delta = 0.00$ mm s^{-1} and $|\Delta E_Q| = 1.72$ mm s^{-1}) attributed to diamagnetic $[Fe(NO)(cyclam\text{-}ac)]^{2+}$ (**4**), the one-electron oxidized product of **3**, based on its Mössbauer parameters reported earlier.[17] However, direct generation of **4** from the reaction of **2** with IBX-ester is unlikely to happen (see below). More importantly, treating independently prepared **3** with a large excess of IBX-ester was found to afford **4** (Supporting Information, Figure S8). All observations thus suggested that newly formed **3** was oxidized to **4** by unreacted IBX-ester in the reaction mixture. Hence, the yield of conversion of **2** to **3** must exceed 90%.

The IR spectrum of the final product generated by the same reaction using ^{15}N–^{14}N–$^{14}N^-$ as the starting material showed two bands at 1901 and 1864 cm^{-1} with nearly identical intensity (Figure 3a). In comparison with the N–O stretching frequency (1903 cm^{-1}) reported for **4**-^{14}NO,[17] the two features can be unambiguously assigned to **4**-^{14}NO and **4**-^{15}NO, respectively, because the measured $^{14}N/^{15}N$ isotope shift of 37 cm^{-1} is in good agreement with that (35 cm^{-1}) predicted by the harmonic oscillator approximation. The ESI-MS spectrum of the reaction product also revealed that the overlapping isotope patterns of **4**-^{4}NO and **4**-^{15}NO have similar intensity (Figure 3b). These findings demonstrated that the N atom in the NO ligand of **3** and **4** originates from the azido ligand of **1**.

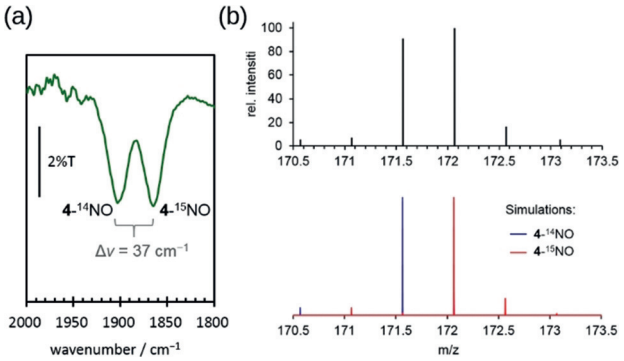

Figure 3. a) IR and b) ESI-MS spectra of the final product generated by the reaction of $^{14}N/^{15}N$ mix-labeled **2** with IBX-ester.

We also examined the reaction of 5 mM of **1** with 100 equiv of trimethylamine oxide (TMAO) in a frozen CH_3CN/MeOH (1:1) solution. The reaction indeed generates **3** albeit with a much lower yield (Scheme 2b, for details, see the Supporting Information). Specifically, EPR and Mössbauer measurements suggested that the yield of **3** is about 2% relative to **1**, and the main product (93%) is $[Fe^{II}(CH_3CN)(cyclam\text{-}ac)]^+$ (**5**),[7] thereby indicating that the OAT process with TMAO cannot compete with the dimerization of **2**.

To gain deep insight into the reaction mechanism, we performed detailed computational investigations. The reactions of **2** with IBX-ester and TMAO to generate **3** were predicted to be highly exothermic by 74.1 and 62.2 kcal mol^{-1}, respectively. In contrast, the theoretical results revealed that the reaction of **2** with IBX-ester to yield **4** possesses a much lower driving force (−15.7 kcal mol^{-1}). Kinetically, the computed potential energy surface (PES) for the OAT process with IBX-ester is always downhill (Supporting Information, Figure S9). Both factors thus render the direct generation of **4** from the reaction of **2** with IBX-ester improbable to occur. Unlike the reaction with IBX-ester, the transformation with TMAO is nearly barrierless, yet with a plateau in the PES upon TMAO approaching the $(FeN)^{2+}$ core (Figure 4a). Note that the dimerization process of **2** features an even higher driving force (ca. −120 kcal mol^{-1}), and the calculated PES shows a constant decrease in energy without a discernible barrier.[7] Therefore, considering the reaction thermodynamics and kinetics, the OAT reaction with IBX-ester has a higher probability than that with TMAO to compete with the self-decay of **2**, when a large excess of the chosen OAT agent was applied. This is why the different outcome was found for the reaction with TMAO and IBX-ester.

As shown in Figure 4c, as the O atom of TMAO approaches the nitrido ligand of **2**, the O 2p based lone pair of TMAO in the Fe–N···O_{TAMO} plane overlaps the unoccupied Fe–N π^*_{xz} MO, which forms the NO σ bonding MO in the end. The other lone pair perpendicular to the Fe–N···O_{TMAO} plane interacts with the singly populated Fe–N π^*_{yz} orbital to generate the N–O π_{op} and π^*_{op} MOs. When the N_{Fe}···O_{TMAO} distance is shortened to 1.52 Å, the O–N σ bond (2.627 Å) in TMAO is essentially broken, thereby resulting in a doubly occupied N 2p based orbital and a vacant O 2p centered orbital (Figure 4b). The former finally evolves to the lone pair

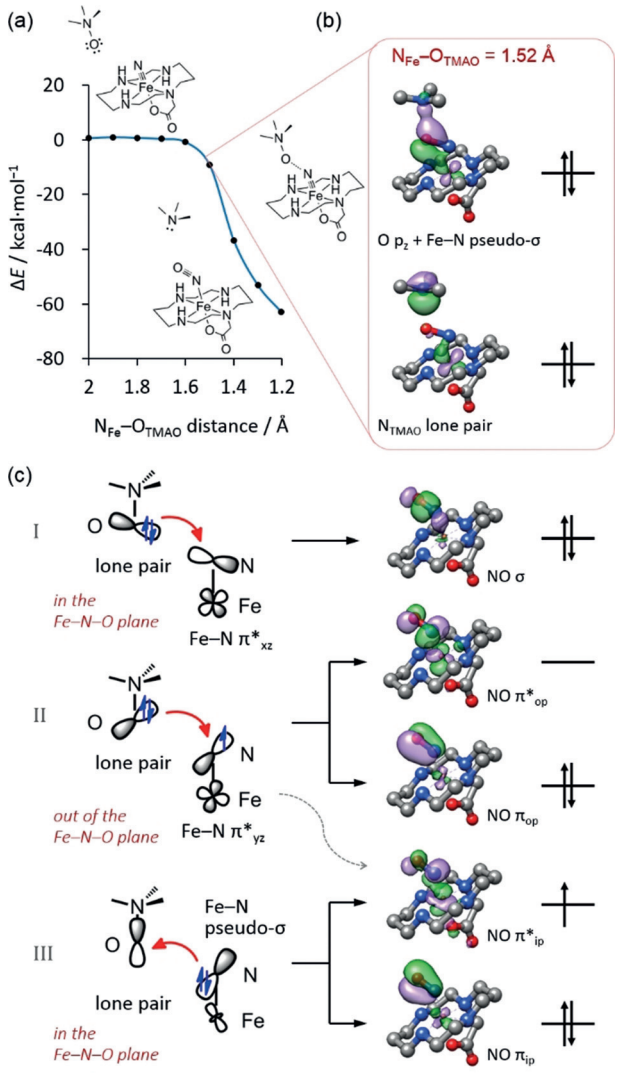

Figure 4. a) Potential energy surface of the reaction of **2** with TMAO computed by a relaxed surface scan of the N_{Fe}–O_{TMAO} distance; b) representative orbitals at the N–O distance of 1.52 Å; c) orbital interactions to form the N–O multiple bonds of **3**.

of trimethylamine, and the latter interacts with the doubly occupied Fe–N pseudo σ-bonding orbital, leading to the in-plane NO π bond. The out-of-plane π interaction involves three electrons, but the unpaired electron in **2** resides in the in-plane NO π^*_{ip} MO rather than NO π^*_{op} as would be expected. As borne out from Figure 4c, the NO π^*_{ip} centered MO is stabilized by the bonding interaction between the NO π^*_{ip} and Fe d_{z^2} fragment orbitals, whereas the NO π^*_{ip} based MO is an antibonding combination with respect to the Fe–NO interaction. Therefore, NO π^*_{ip} MO has lower energy than NO π^*_{op}.[17]

In summary, during the reaction of **2** to **3**, the OAT agent essentially donates a closed-shell singlet O atom to **2**, and the $(FeN)^{2+}$ unit functions not only as an electron acceptor but also an electron donor. Therefore, the reaction does not follow a radical-coupling mechanism as postulated for the N_2 expulsion,[7,16] but reveals the ambiphilic nature of **2** found for related diamagnetic metal nitrides.[19] Consequently, the synergetic orbital interactions accompanied by the mutual electron transfer between **2** and the O-atom donor build up N–O multiple bonds in a concerted yet asynchronous way without an intervening intermediate. On the basis of the above analysis, the oxygenation of closed-shell metal nitrides should follow a similar mechanism. This work enriches the already diversified reactivity of high-valent iron nitrides and provides a different viable strategy for constructing multiple bonds for diatomic molecules.

Acknowledgements

We gratefully acknowledge the financial support from the Max-Planck Society, in particular, the Joint Work Space of MPI-CEC and MPI-KOFO, and the Ministry of Science and Technology of Taiwan (MOST 105-2113-M-003-005-MY3 to W.-Z.L.). W.-Z.L. and S.Y. also acknowledge the MOST-DAAD Project-Based Personnel Exchange Program (MOST 107-2911-I-003-502 and DAAD 57320810).

Conflict of interest

The authors declare no conflict of interest.

Keywords: EPR spectroscopy · iron · Mössbauer spectroscopy · nitrides · nitrosyl

How to cite: *Angew. Chem. Int. Ed.* **2019**, *58*, 17589–17593
Angew. Chem. **2019**, *131*, 17753–17757

[1] a) B. M. Hoffman, D. Lukoyanov, Z.-Y. Yang, D. R. Dean, L. C. Seefeldt, *Chem. Rev.* **2014**, *114*, 4041–4062; b) H. Tanaka, K. Arashiba, S. Kuriyama, A. Sasada, K. Nakajima, K. Yoshizawa, Y. Nishibayashi, *Nat. Commun.* **2014**, *5*, 3737; c) G. Ertl, *Angew. Chem. Int. Ed.* **2008**, *47*, 3524–3535; *Angew. Chem.* **2008**, *120*, 3578–3590.

[2] a) C. J. Weststrate, J. W. Bakker, A. C. Gluhoi, W. Ludwig, B. E. Nieuwenhuys, *Catal. Today* **2010**, *154*, 46–52; b) W. D. Mieher, W. Ho, *Surf. Sci.* **1995**, *322*, 151–167.

[3] a) J. M. Smith, D. Subedi, *Dalton Trans.* **2012**, *41*, 1423–1429; b) C. T. Saouma, J. C. Peters, *Coord. Chem. Rev.* **2011**, *255*, 920–937; c) J. F. Berry, *Comments Inorg. Chem.* **2009**, *30*, 28–66; d) J. Hohenberger, K. Ray, K. Meyer, *Nat. Commun.* **2012**, *3*, 720–713; e) J. Cheng, L. Wang, P. Wang, L. Deng, *Chem. Rev.* **2018**, *118*, 9930–9987.

[4] a) J. M. Smith in *Progress in Inorganic Chemistry, Vol. 58* (Ed.: K. D. Karlin), Wiley, Hoboken, **2014**, pp. 417–470; b) J. Cheng, L. Wang, P. Wang, L. Deng, *Chem. Rev.* **2018**, *118*, 9930–9987; c) R. A. Eikey, M. M. Abu-Omar, *Coord. Chem. Rev.* **2003**, *243*, 83–124.

[5] a) J. J. Scepaniak, C. S. Vogel, M. M. Khusniyarov, F. W. Heinemann, K. Meyer, J. M. Smith, *Science* **2011**, *331*, 1049–1052; b) J. J. Scepaniak, J. A. Young, R. P. Bontchev, J. M. Smith, *Angew. Chem. Int. Ed.* **2009**, *48*, 3158–3160; *Angew. Chem.* **2009**, *121*, 3204–3206; c) T. A. Betley, J. C. Peters, *J. Am. Chem. Soc.* **2004**, *126*, 6252–6254.

[6] For selected examples, see: a) J. J. Scepaniak, R. P. Bontchev, D. L. Johnson, J. M. Smith, *Angew. Chem. Int. Ed.* **2011**, *50*, 6630–6633; *Angew. Chem.* **2011**, *123*, 6760–6763; b) A. K. Maity, J. Murillo, A. J. Metta-Magaña, B. Pinter, S. Fortier, *J. Am. Chem. Soc.* **2017**, *139*, 15691–15700.

[7] O. Krahe, E. Bill, F. Neese, *Angew. Chem. Int. Ed.* **2014**, *53*, 8727 – 8731; *Angew. Chem.* **2014**, *126*, 8872 – 8876.
[8] H.-C. Chang, B. Mondal, H. Fang, F. Neese, E. Bill, S. Ye, *J. Am. Chem. Soc.* **2019**, *141*, 2421 – 2434.
[9] G. E. Cutsail III, B. W. Stein, D. Subedi, J. M. Smith, M. L. Kirk, B. M. Hoffman, *J. Am. Chem. Soc.* **2014**, *136*, 12323 – 12336.
[10] a) M. Schlangen, J. Neugebauer, M. Reiher, D. Schröder, J. P. López, M. Haryono, F. W. Heinemann, A. Grohmann, H. Schwarz, *J. Am. Chem. Soc.* **2008**, *130*, 4285 – 4294; b) G. Sabenya, L. Lázaro, I. Gamba, V. Martin-Diaconescu, E. Andris, T. Weyhermüller, F. Neese, J. Roithová, E. Bill, J. Lloret-Fillol, M. Costas, *J. Am. Chem. Soc.* **2017**, *139*, 9168 – 9177.
[11] a) J. Torres-Alacan, O. Krahe, A. C. Filippou, F. Neese, D. Schwarzer, P. Vöhringer, *Chem. Eur. J.* **2012**, *18*, 3043 – 3055; b) J. Torres-Alacan, U. Das, A. C. Filippou, P. C. Vöhringer, *Angew. Chem. Int. Ed.* **2013**, *52*, 12833 – 12837; *Angew. Chem.* **2013**, *125*, 13067 – 13071.
[12] W.-T. Lee, R. A. Juarez, J. J. Scepaniak, S. B. Muñoz III, D. A. Dickie, H. Wang, J. M. Smith, *Inorg. Chem.* **2014**, *53*, 8425 – 8430.
[13] N. Aliaga-Alcalde, S. DeBeer George, B. Mienert, E. Bill, K. Wieghardt, F. Neese, *Angew. Chem. Int. Ed.* **2005**, *44*, 2908 – 2912; *Angew. Chem.* **2005**, *117*, 2968 – 2972.
[14] For selected examples, see: a) A. Walstrom, M. Pink, H. Fan, J. Tomaszewski, K. G. Caulton, *Inorg. Chem.* **2007**, *46*, 7704 – 7706; b) X.-Y. Yi, T. C. H. Lam, Y.-K. Sau, Q.-F. Zhang, I. D. Williams, W.-H. Leung, *Inorg. Chem.* **2007**, *46*, 7193 – 7198.
[15] For selected examples, see: a) D. S. Williams, T. J. Meyer, P. S. White, *J. Am. Chem. Soc.* **1995**, *117*, 823 – 824; b) T. J. Crevier, S. Lovell, J. M. Mayer, A. L. Rheingold, I. A. Guzei, *J. Am. Chem. Soc.* **1998**, *120*, 6607 – 6608.
[16] For selected examples, see: a) M. G. Scheibel, B. Askevold, F. W. Heinemann, E. J. Reijerse, B. de Bruin, S. Schneider, *Nat. Chem.* **2012**, *4*, 552 – 558; b) J. Schöffel, A. Y. Rogachev, S. DeBeer George, P. Burger, *Angew. Chem. Int. Ed.* **2009**, *48*, 4734 – 4738; *Angew. Chem.* **2009**, *121*, 4828 – 4832.
[17] R. G. Serres, C. A. Grapperhaus, E. Bothe, E. Bill, T. Weyhermüller, F. Neese, K. Wieghardt, *J. Am. Chem. Soc.* **2004**, *126*, 5138 – 5153.
[18] J. H. Enemark, R. D. Feltham, *Coord. Chem. Rev.* **1974**, *13*, 339 – 406.
[19] a) J. J. Scepaniak, C. G. Margarit, J. N. Harvey, J. M. Smith, *Inorg. Chem.* **2011**, *50*, 9508 – 9517; b) F. S. Schendzielorz, M. Finger, C. Volkmann, C. Würtele, S. Schneider, *Angew. Chem. Int. Ed.* **2016**, *55*, 11417 – 11420; *Angew. Chem.* **2016**, *128*, 11589 – 11592; c) S. B. Seymore, S. Brown, *Inorg. Chem.* **2002**, *41*, 462 – 469; d) J. Schöffel, N. Šušnjar, S. Nückel, D. Sieh, P. Burger, *Eur. J. Inorg. Chem.* **2010**, 4911 – 4915; e) J. Abbenseth, M. Finger, C. Würtele, M. Kasanmascheff, S. Schneider, *Inorg. Chem. Front.* **2016**, *3*, 469 – 477.

Manuscript received: July 12, 2019
Revised manuscript received: September 10, 2019
Accepted manuscript online: September 18, 2019
Version of record online: October 21, 2019

